



Starch-Based Bioplastic Reinforced by Cellulose Nanocrystal Isolated from Water Hyacinth

Fauziah Rismawati^{1,✉}, Feronika Heppy Sriherfyna¹, Firda Aulya Syamani²

DOI: <https://doi.org/10.15294/jbat.v12i1.40239>

¹Department of Food Science and Biotechnology, Faculty of Agricultural Technology, Brawijaya University, Jl. Veteran, Ketawanggede, Kec. Lowokwaru, Malang City, East Java 65145, Indonesia

²Biomass and Bioproduct Research Center, National Research and Innovation Agency, Jl. Raya Jakarta-Bogor No.KM. 46, Cibinong, Bogor Regency, West Java 16911, Indonesia

Article Info

Article history:

Received

19 November 2022

Revised

05 December 2022

Accepted

31 December 2022

Online

17 January 2023

Keywords:

CNC;

Starch Bioplastic;

Water Hyacinth

Abstract

This study aims to determine the effect of the addition of cellulose nanocrystals (CNC) with different concentrations (0,2,4,6,8,10%) isolated from water hyacinth on tensile strength, elongation, and biodegradability of corn starch bioplastics. CNC isolation was conducted, including alkalization, bleaching, acid hydrolysis, and sonication. After the isolation process, CNC was characterized based on functional group, crystallinity, and morphology surface. Then, the production of starch bioplastic using solution casting was carried out with the addition of CNC. The results showed chemical treatments affected the functional group, increasing the crystallinity index, and removing the fibril structure in water hyacinth fibers. Likewise, the addition of CNC to starch bioplastic fluctuated the tensile strength and elongation. In the biodegradability test, the physical appearance of the bioplastic completely changed. Then, the optimum mass reduction occurred in the 6% CNC on the 10th day.

INTRODUCTION

The petroleum-based plastics production drastically increased, from 2 million tonnes in 1950 to 381 million tonnes in 2015 (Ritchie & Roser, 2018). It occurs due to the plastic characteristics, which are compatible, lightweight, and adaptable to variations of applications such as packaging, medical equipment, and automobile. Although plastics have many advantages, it pollutes the environment since it is difficult to degrade biologically. Plastic waste, for example, has been discovered in the digestive organs of dead seabirds and fish. Moreover, poor waste management exacerbates the plastic waste problem. Only 9% of plastic was recycled, 12% burned, and 80% accumulated in landfills from 1950 to 2015 (OECD, 2018).

Starch bioplastic, which uses renewable resources and is more environmentally friendly, could be an alternative substitute for petroleum-based plastic. However, its mechanical properties are poor compared to plastic. The reinforcing agent could be applied to starch bioplastic to improve mechanical properties. Cellulose nanocrystals are excellent reinforcing agents, having high crystallinity, biocompatibility, and biodegradability (Xie et al., 2018).

In this study, CNC was isolated from water hyacinth (WH), a free-floating aquatic weed with a cellulose content of 60% (Abdel-Fattah & Abdel-Naby, 2012). We explored WH as a raw material for CNC isolation, whereas previous studies used non-wood lignocellulose, wood resources, and agricultural waste or byproducts (Owoyokun et al., 2021). Another reason is to reduce the environmental effect caused by the dense

✉ Corresponding author:
E-mail: fauziah16@student.ub.ac.id

population of WH in the aquatic ecosystem. For example, WH could decrease dissolved oxygen in water, interfere with the fish's life, and hinder water transportation (Villamagna & Murphy, 2010). Besides reducing its effects, WH is abundant in nature since its growth massively, and it would be advantageous as raw material. Subsequently, CNC is added to starch bioplastic to study its effect on the starch bioplastic's tensile strength, elongation, and biodegradability.

MATERIALS AND METHODS

Materials

NaOH (Merck), H₂O₂ 30% (Wako), HCl 37% (Merck), Corn Flour (Maizenaku), Glycerol 85% (Merck), Acetic Acid (Wako), Reverse Osmosis Water (RO), Aquades, and soils.

Methods

Alkalization

Fifty grams of water hyacinth fiber in powder form were reacted in 700 mL of 10% NaOH solution at 65°C for two hours. Afterward, the alkalinized fiber was rinsed with RO water until the pH was 8 or 9.

Bleaching

The alkalinized fiber was reacted in 500 mL H₂O₂ 30% at 60°C for an hour. Then, the samples were rinsed with RO water until pH 7.

Acid Hydrolysis

The bleached fibers were reacted in 750 mL of 5 M HCl at 60°C for 1 hour in a fume hood. After the reaction was complete, the hydrolyzed fibers were put into a 50 mL centrifuge tube and centrifuged at 2000 rpm and 9°C for 30 minutes. Then, the solids were filtered and rinsed until the pH was neutral.

Sonication

In 100 mL of RO water, a half-gram sample was added. Following that, sonication was performed for an hour at a power and pulse of 30% respectively. Afterward, the CNC is evaporated and filtered.

Bioplastic Production

The CNC was dispersed first for 15 minutes using sonication and homogenized at 200

rpm at room temperature for 30 minutes. After that, it was heated at 50-60°C. Then, starch was added and stirred using a magnet at 200 rpm at 70-80°C or until the gelatinization occurred. Then, added glycerol and acetic acid and homogenized for 30 minutes. Poured the bioplastic gels into the mold and left it for 5 to 7 days at room temperature.

Functional Group Analysis

Infrared spectra of water hyacinth fiber, alkalization, bleaching, acid hydrolysis, and sonication were recorded by the Shimadzu FTIR instrument at Chemistry Department FMIPA UB. With a resolution of 4 cm⁻¹, the wave numbers employed range from 400 to 4500 cm⁻¹.

Crystallinity Index

The instrument used is the Shimadzu MAXima X XRD-7000 Integrated Laboratory of Bioproduct, Research Center for Biomass and Bioproducts-BRIN. The sample is a 100 mesh solid powder. In addition, the current and voltage used are 40 kV and 30 mA. Then, the diffraction intensity range was measured at (2θ = 10 - 30°).

$$CI (\%) = \frac{I_{200} - IAM}{IAM} \times 100 \quad (1)$$

Where a I₂₀₀ is intensity maximum of crystalline region at 2θ = ~22° and IAM is intensity amorphous region 2θ = ~18°.

Morphological Analysis

The morphology of CNC was observed using the FESEM Thermo Scientific Quattro S Integrated Laboratory of Bioproduct, Research Center for Biomass and Bioproducts-BRIN. The sample is in the form of 100 mesh powder. The magnifications used are 500x, 1500x, and 5000x with an accelerating voltage of 1 kV.

Tensile Strength and Elongation Test

Mechanical properties such as tensile strength and elongation of bioplastics were tested using the Universal Testing Machine AGS-X Shimadzu Integrated Laboratory of Bioproduct, Research Center for Biomass and Bioproducts-BRIN. The speed used is 30 mm/minute and a capacity of 5 kN. The sample is in the form of a thin plate with an average length, width, and thickness of 84.78 mm, 19.52, and 0.36 mm, respectively.

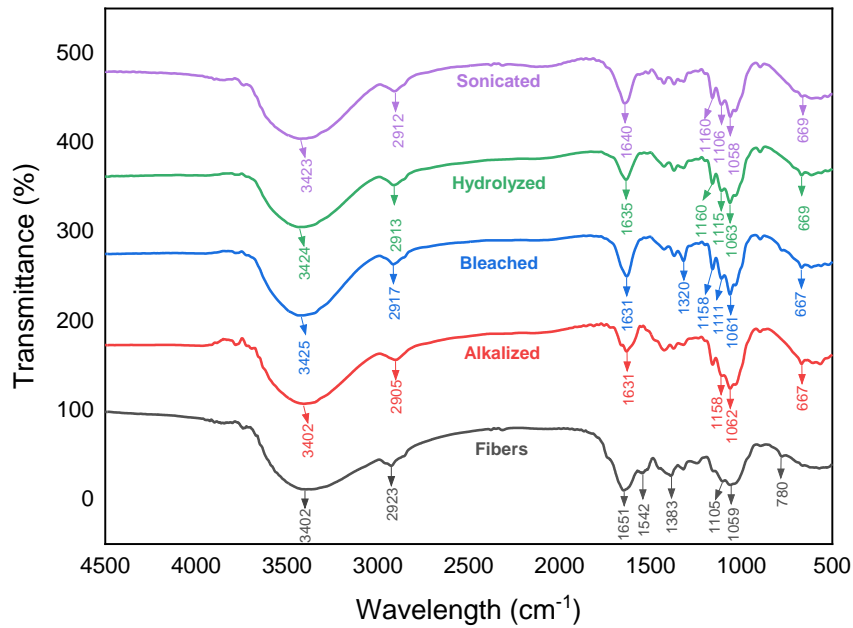


Figure 1. Infrared spectrum of FTIR analysis.

Soil Burial Test

The biodegradability test procedure is a modification of the research of Nissa et al. The soil used is an organic fertilizer which is then air-dried for 5 days to reduce water content. The soil is placed in a transparent plastic poly bag that is airtight and has no holes under the polybag. Bioplastic samples measuring 2 x 2 cm were buried in the soil to a depth of 7 cm. Observations were made every 2 days for 10 days. The indicators to be considered are changes in mass and physical changes such as cracks and color.

$$\text{Mass Reduction} = \frac{W_0 - W_t}{W_0} \times 100 \quad (3)$$

Where W_0 is the initial mass of bioplastic and W_t is bioplastic mass on the day of biodegradability testing.

RESULTS AND DISCUSSION

Functional Group Analysis

Water hyacinth powder, alkalization, bleaching, acid hydrolysis, and sonication were used for FTIR analysis. Figure 1 shows a broad peak between 3200 and 3500 cm^{-1} , indicating the presence of an OH stretching vibration. There is also a medium-sized peak between 2800 and 3000 cm^{-1} that represents a CH symmetrical stretching vibration. These findings, which correspond with

Asrofi et al. (2017) and Packiam et al. (2021), indicate the existence of the cellulose molecule.

All samples have a spectrum ranging from 1500 to 1600 cm^{-1} , corresponding to the vibrations caused by water absorption. Water hyacinth fiber has the most water absorption due to the amorphous areas. The water absorption's vibration decreased after the chemical treatment, indicating the loss of the amorphous region (Asrofi et al., 2017). There are also spectrum reductions at 1651 cm^{-1} and 1383 cm^{-1} , showing C=O group stretching vibrations on aromatic compounds and OH bending vibrations on OH phenolic compounds in lignin. Similar to Asrofi et al. (2017), the absorption at the peaks of 1253, 1322, and 1620 cm^{-1} was reduced, as a result of alkalization and bleaching, which disrupted the bond and reduced absorption. Then, similar to Packiam et al. (2021), there is a peak at 1059 cm^{-1} indicating the C-O-C glycosidic ether bond stretching vibration in the polysaccharide molecule (Nikonenko et al., 2000; Packiam et al., 2021).

Crystallinity Index

The crystallinity index (CI) of all the samples is seen in Table 1. The chemical treatment increased the CI through the amorphous removal of lignin and hemicellulose without affecting much the crystal structure. However, the CI decreased after the sonication treatment, as seen in Figure 2. The intensity decreased due to the intense cavitation acoustics from sonication, which could destroy the

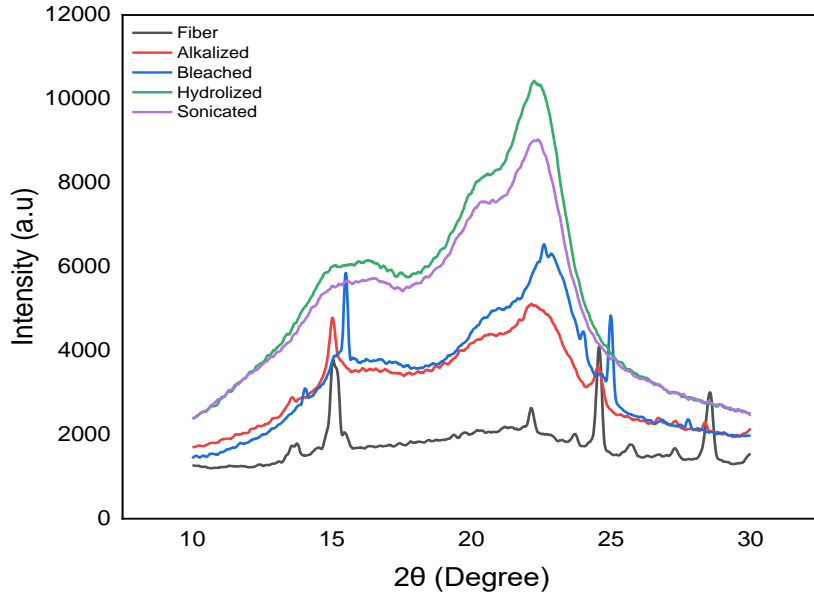


Figure 2. XRD pattern.

Table 1. Crystallinity index of samples.

Sampels	Crystallinity Index (%)
Fiber	33.58
Alkalized	33.60
Bleached	45.51
Acid Hydrolized	45.08
Sonicated	40.03

crystalline cellulose partially. Another factor that caused the decrease in CI is the longer sonication duration, for example, the CI value dropped by 12% in Shojaeianani et al. (2020) study. In addition, the CI in this study is much lower than others. Asrofi et al. (2017) and Oyeoka et al. (2021) isolated the CNC from water hyacinth, of which the CI had been 73% and 72% respectively. It could be improved by a potential solution, such as optimizing the sonication and hydrolyzed time.

Morphological Analysis

Figure 3 shows the picture of SEM analysis on CNC samples with three different magnifications. It can be seen that no visible fibril structure, indicating that the alkalization and bleaching successfully removed the lignin and hemicellulose (Sainorudin, 2021). However, in this work, the detail of the CNC surface cannot be seen clearly. It is caused by the accelerating voltage (AV) below 5 kV. To resolve this, applying high-voltage AV could be an alternative, but the sample must be gold-coated to prevent damage. According to Khan et al. (2021), they utilized a voltage of 15-20 kV, allowing the

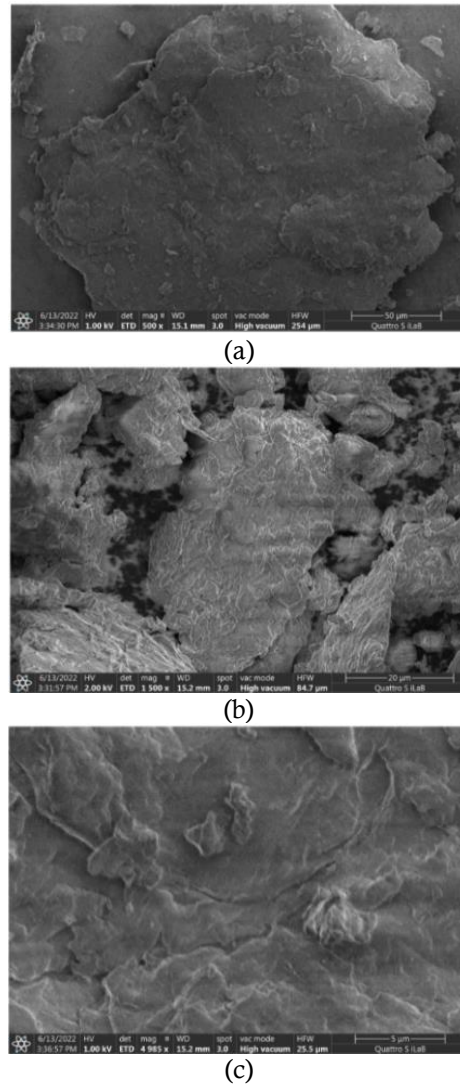


Figure 3. Morphology of CNC with magnifications (a) 500x; (b) 1500x; and (c) 5000x.

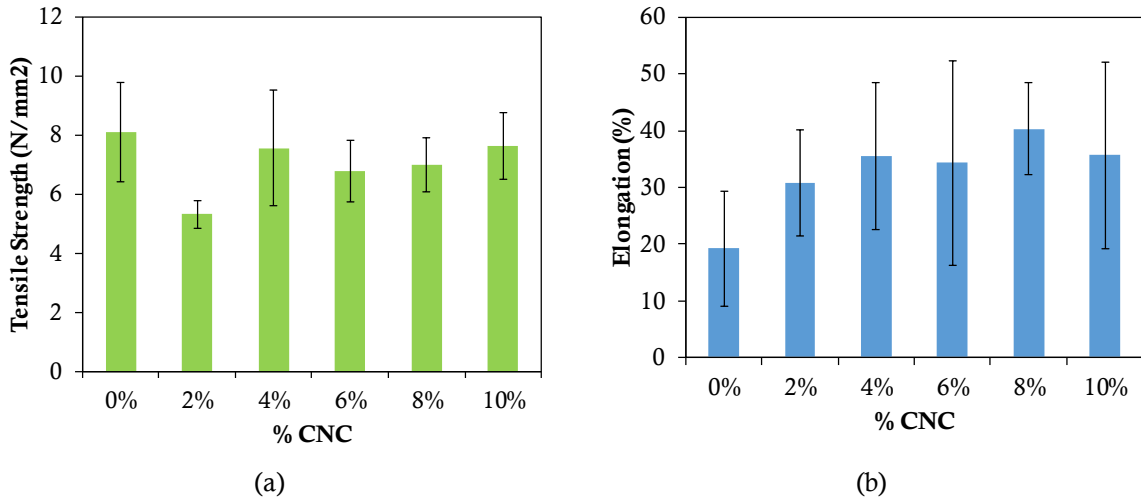


Figure 4. Tensile strength and elongation of starch bioplastic reinforced by different concentrations of CNC.

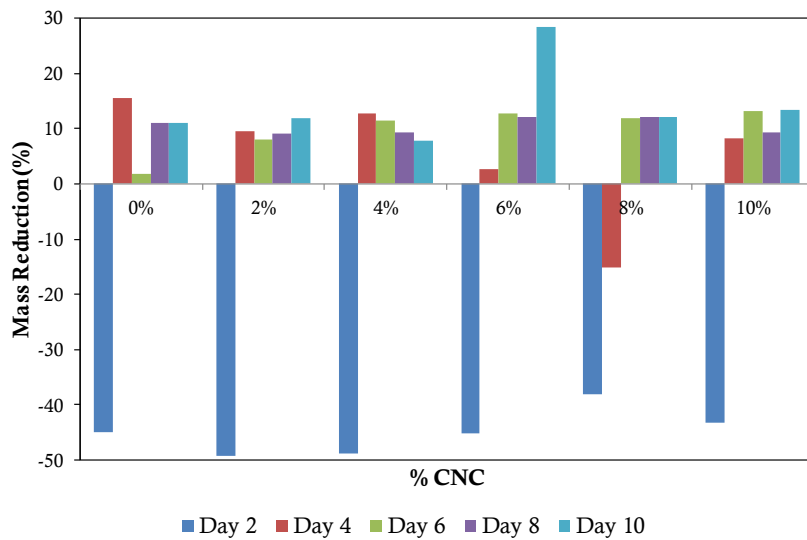


Figure 5. Mass reduction of bioplastic underwent soil burial test.

surface detail of the CNC to be visible, namely the needle-structured CNC aggregated due to the strong hydrogen bonding in CNC.

Tensile Strength and Elongation

The tensile strength of CNC from 2% to 10% was slightly lower than the CNC 0%. The highest elongation was CNC at 8%, while CNC at 0% was the lowest. In this study, the addition of CNC was not slightly affected the tensile strength and elongation. For instance, Arbanah et al. (2019) produced bioplastic reinforced with CNC isolated from mangosteen peel, and the highest tensile strength was CNC at 0%. Another example is Zainuddin et al (2013), which studied the addition of CNC isolated from kenaf fiber to bioplastic. The result, as the concentration of CNC increased, so did the tensile strength. The highest tensile strength

was CNC 6% at 8.2 MPa. Because of CNC agglomeration and poor dispersion, CNC concentrations above 6% did not increase tensile strength. Aside from CNC agglomeration and poor dispersion, the addition of starch powder at 50-60°C reduced tensile strength. To address this, CNC suspension is added to the gelatinized starch (Agustin et al., 2014; Johar & Ahmad, 2012).

Soil Burial Test

Figure 5 represents the physical change of bioplastics for ten days of soil burial. Before the bioplastics were buried, the appearance was transparent, but bioplastics reinforced by CNC looked rougher at the surface. Every two days of observation, the bioplastics' appearance altered to browner, and there were cracks on their surface. Also, the black dot spotted on bioplastics indicated

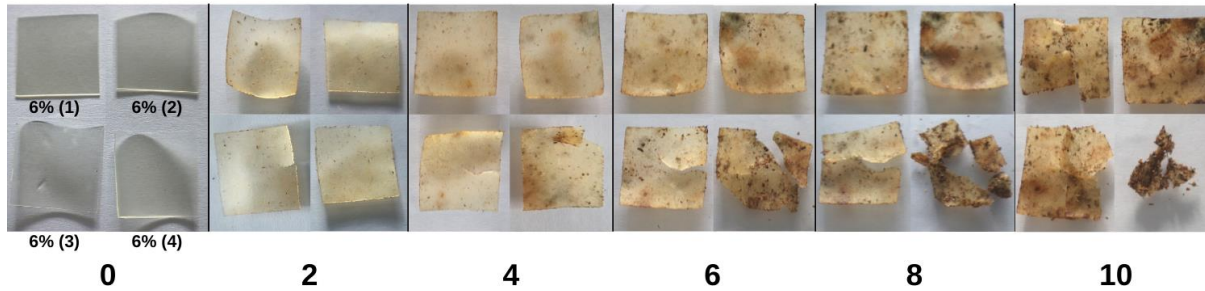


Figure 6. Physical changes of bioplastic reinforced by CNC 6% underwent soil burial test

the growth of microorganisms. Likewise, Figure 6 depicts the mass reduction of bioplastics. The mass fluctuated due to the bioplastics' hydrophilic characteristic, absorbing water in the soil. In addition, the black dot also influenced the mass of bioplastics. The results of this study are quite different of Nissa et al. (2019). Their results showed that mass reduced consistently. The longer the testing time, the mass of the bioplastic decreased. On the 10th day of the biodegradability test, their mass reduction reached 29.89%.

CONCLUSION

Successful completion of the CNC characterization based on functional groups revealed the final product as cellulose. In addition, chemical treatment can increase crystallinity and loss of fibril structure. The addition of CNC did not significantly increase the tensile strength and elongation values in bioplastics due to poor dispersion. After then, bioplastics experienced physical change, including cracking, fading, and microbial growth. In addition, the bioplastic's mass increased due to its hydrophilic nature.

ACKNOWLEDGEMENT

The authors acknowledge the facilities, scientific and technical support from Advanced Characterization Laboratories Cibinong – Integrated Laboratory of Bioproduct, National Research and Innovation Agency through E-Layanan Sains, Badan Riset dan Inovasi Nasional (BRIN).

REFERENCES

Abdel-Fattah, A. F., Abdel-Naby, M. A. 2012. Pretreatment and Enzymic Saccharification of Water Hyacinth

Cellulose. *Carbohydrate Polymers*. 87(3): 2109-2113.

Agustin, M. B., Ahmmad, B., Alonzo, S. M. M., Patriana, F. M. 2014. Bioplastic Based on Starch and Cellulose Nanocrystals from Rice Straw. *Journal of Reinforced Plastics and Composites*. 33(24): 2205-2213.

Arbanah, M., Roslan, A., Sanusi, S. N. A., Shahimi, M. Q., Nazari, N. Z. 2019. Mechanical Properties of Bioplastic Form Cellulose Nanocrystal (CNC) Mangosteen Peel Using Glycerol as Plasticizer. *Journal of Physics: Conference Series*. 1349: 012099.

Asrofi, M., Abrial, H., Kasim, A., Pratoto, A. 2017. XRD and FTIR Studies of Nanocrystalline Cellulose from Water Hyacinth (*Eichornia Crassipes*) Fiber. *Journal of Metastable and Nanocrystalline Materials*. 29: 9–16.

Johar, N., & Ahmad, I. 2012. Morphological, Thermal, and Mechanical Properties of Starch Biocomposite Films Reinforced by Cellulose Nanocrystals from Rice Husks. *BioResources*. 7(4): 5469–77.

Khan, A., Jawaid, M., Kian, L. K., Khan, A. A. P., Asiri, A. M. 2021. Isolation and Production of Nanocrystalline Cellulose from *Conocarpus* Fiber. *Polymers*. 13(11): 1835.

Nikonenko, N. A., Buslov, D. K., Zhbankov, R. G., Sushko, N. I. 2000. Investigation of Stretching Vibrations of Glycosidic Linkages in Disaccharides and Polysaccharides with Use of IR Spectra Deconvolution. *Peptide Science*. 57(4): 257-262.

Nissa, R. C., Fikriyyah, A. K., Abdullah, A. H. D., Pudjiraharti, S. 2019. Preliminary Study of Biodegradability of Starch-Based Bioplastics Using ASTM G21-70, Dip-Hanging, and Soil Burial Test Methods.

- IOP Conference Series: Earth and Environmental Science. 277(1): 012007.
- OECD. 2018. Improving Plastics Management : Trends, Policy Responses, and the Role of International Co-Operation and Trade | OECD Environment Policy Papers | OECD ILibrary. Paris.
- Oyeoka, H. C., Ewulonu, C. M., Nwuzor, I. C., Obele, C. M., Nwabanne, J. T. 2021. Packaging and degradability properties of polyvinyl alcohol/gelatin nanocomposite films filled water hyacinth cellulose nanocrystals. *Journal of Bioresources and Bioproducts*. 6(2): 168–185.
- Owoyokun, T., Berumen, C. M. P., Luévanos, A. M., Cantú, L., Cenicerros, A. C. L. 2021. Cellulose Nanocrystals: Obtaining and Sources of a Promising Bionanomaterial for Advanced Applications. *Biointerface Research in Applied Chemistry*. 11(4): 11797-11816.
- Packiam, K. K., Murugesan, B., Sundaramoorthy, P. M. K., Srinivasan, H., Dhanasekaran, K. 2021. Extraction, Purification and Characterization of Nanocrystalline Cellulose from Eichhornia Crassipes (Mart.) Solms: A Common Aquatic Weed Water Hyacinth. *Journal of Natural Fibers*. 19(14): 7424-7435.
- Ritchie, H., Roser, M. 2018. Plastic Pollution - Our World in Data. Retrieved July 16, 2022 (<https://ourworldindata.org/plastic-pollution>).
- Sainorudin, M. H., Abdullah, N. A., Rani, M. S. A., Mohammad, M., Mahizan, M., Shadan, N., Abd Kadir, N. H., Yaakob, Z., El-Denglawey, A., Alam, M. 2021. Structural characterization of microcrystalline and nanocrystalline cellulose from Ananas comosus L. leaves: Cytocompatibility and molecular docking studies. *Nanotechnology Reviews*. 10(1): 793–806.
- Shojaeianani, J., Bajwa, D., Holt, G. 2020. Sonication amplitude and processing time influence the cellulose nanocrystals morphology and dispersion. *Nanocomposites*. 6(1): 41–46.
- Villamagna, A. M. & Murphy, B. R. 2010. Ecological and socio-economic impacts of invasive water hyacinth (*Eichhornia crassipes*): a review. *Freshwater Biology*. 55(2): 282-298.
- Xie, S., Zhang, X., Walcott, M. P., Lin, H. 2018. Cellulose Nanocrystals (CNCs) Applications: A Review. *Engineered Science*. 2:4–16.
- Zainuddin, S. Y. Z., Ahmad, I., Kargarzadeh, H., Abdullah, I., Dufresne, A. 2013. Potential of Using Multiscale Kenaf Fibers as Reinforcing Filler in Cassava Starch-Kenaf Biocomposites. *Carbohydrate Polymers*, 92(2):2299–2305.